Tensile Testing of Microsamples

by D. A. LaVan and W. N. Sharpe, Jr.

ABSTRACT—Structural analysis has advanced rapidly to the point where lack of knowledge about the local inhomogeneity and anisotropic nature of the materials prevents the accurate prediction of the behavior; models can incorporate local material properties provided they can be experimentally determined. Conventional tensile techniques are unable to test specimens from submillimeter-sized regions, and microhardness measurements do not reveal directional variations. A system has been developed to perform tensile tests on microsamples that are 3.1 mm long with a gage cross section that is 0.2 mm square. The volume of the test region is roughly 500,000 times smaller than a standard half-inch diameter specimen. Tensile stress-strain curves are measured, and the yield strength, ultimate strength, modulus and elongation are calculated for each sample. Samples cut from the weld metal of undermatched welds in HY-100 plate showed a large variation in properties from the center of the weld to the outer edge, as well as anisotropy at some locations. The average mechanical properties of a group of microsamples cut from the outer region of the weldment compared favorably with measurements made using full-sized specimens; the variation in the microsample measurements reflect local variations in the material that are not measured with full-sized specimens.

KEY WORDS—Micro, mechanics, properties, tensile, steel

The use of undermatched welding to fabricate structures from 690 MPa and stronger steels has led to interest in characterizing the local properties of the weld metal. Conventional tensile techniques are unable to sample sufficiently small regions, and microhardness indentations do not identify directional variations.

The design, cutting and preparation of a microsample is described. During the test, strain is measured directly on two sides of the specimen using laser interferometry and the load is measured using a commercial load cell. The movable grip is supported by a linear air bearing. The physical dimensions of the specimen are measured using the calibrated eyepiece of a microhardness test machine.

Results of more than 80 microsamples tested from two undermatched welds in HY-100 plate are presented and compared to average properties determined from conventional, full-sized, tensile samples.

D. A. LaVan (SEM Member) is a Postdoctoral Fellow, Sandia National Laboratories, Albuquerque, NM 87185. W. N. Sharpe, Jr., (SEM Member) is Decker Professor, Department of Mechanical Engineering, Johns Hopkins University, Baltimore, MD 21218.

Original manuscript submitted: July 30, 1998.
Final manuscript received: February 1, 1999.

Specimen Design

Gripping small specimens may be among the most challenging of the tasks associated with miniature sample testing. Small misalignments create large bending strains, and gripping can easily alter or destroy the sample under investigation. Gluing small specimens to the grips is always an option, as long as the adhesive shear area is large compared to the cross section of the specimen. However, this precludes rapid successive tests, since appropriate adhesives have long cure times and often longer debonding times. Because of these concerns, a classic bow-tie-shaped specimen was chosen that fits into tapered grips, is self-aligning and requires no clamping or gluing of the sample. Figure 1 is a drawing of the specimen. The radius of curvature in the gage section is 9.4 mm; the gage length is 300 μm with nominal gage cross-section dimensions of 200 μm by 200 μm. The handbook value for the stress concentration factor of the center radius is 1.01,[1] which was confirmed with a simple ABAQUS model. The tapers on the ends are designed to fit the matching tapers in the grips, and a fillet between the center section and the taper reduces the stress concentration.

Test Machine Design

There are four major components in a tensile test machine: the mechanical frame and grips, the displacement actuator, the load sensor and the strain sensors. To successfully test microspecimens, these components must be consistent with the small scale of the sample. The design of conventional-size testing machines is not significantly concerned with friction in the grips and reinforcement of the specimen due to the strain or clip gages. For microsamples, these are difficult obstacles.

The sample fits into a cutout in the grip; a small machine screw captures the sample but does not compress or twist it. Friction is overcome by mounting the movable grip to a linear air bearing. The air-bearing slide cross section is 12 mm wide by 10 mm deep.

Displacement is provided by a motorized dovetail slide. This unit is gear reduced to rotate the lead screw between 0.2 to 2.0 rpm. The screw has a pitch of 0.635 mm (40 tpi); the displacement rate is 0.12 to 1.2 mm per minute. Consequently, the nominal strain rate, for a sample with gage length of 300 μm, can be adjusted within the range of 0.007 to 0.07 s^{-1}. The load is transferred to the movable grip via a 250 mm long steel wire with a diameter of 0.45 mm; the compliance of the wire reduces the effective strain rate by roughly one order of magnitude.

The test machine is constructed on top of an optical breadboard placed on a heavy steel table. No special vibration

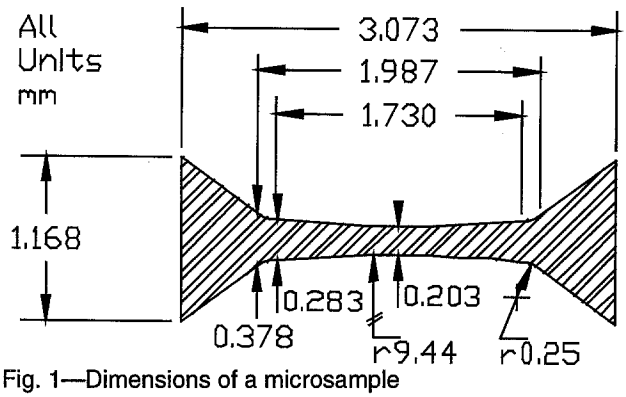

Fig. 1—Dimensions of a microsample

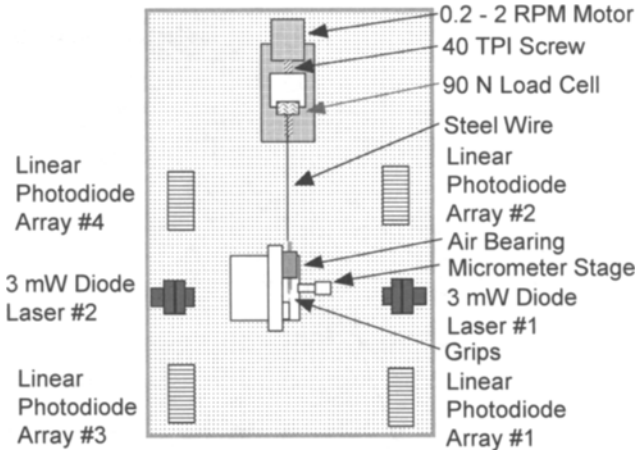

Fig. 2—Top view of the machine layout

isolation is used. The sample and grip assembly sits in the center of the table, a diode laser illuminates the strain markers on each side and a pair of linear photodiodes detects the fringe patterns from each side of the specimen. The sensors are typically 250 mm from the sample. Figure 2 shows a top view of the machine layout. Figure 3 shows a photograph of a sample in the grips and the air bearing.

Load is measured using a commercial 90-N (20-lb) load cell connected to a signal conditioner and digital readout that provide a voltage output proportional to the load. The output of the load cell is 2.86 mV per N, whereas the input range for the signal conditioner is set to 0-200 mV. This limits the usable range to 70 N but maximizes the sensitivity at low loads. The typical ultimate load for one of the steel samples is about 50 N, which is well within the central 70 percent of the load range suggested by ASTM standards. The stand-alone commercial load cell was calibrated by removing the load cell from the machine and verifying the output with precision weights.

The interferometric strain/displacement gage (ISDG) is used to measure strain on both sides of the sample. The principles of this technique are shown in Fig. 4 and discussed in detail in Refs. 2-4. It is important to recognize that this system accomplishes three objectives. First, it is nonreinforcing; this means that nothing has to be attached to the sample to measure the strain. The thickness of a resistive strain gage is large when compared to such a small sample, and any technique in which the gage is attached to the sample would yield false readings that reflect the combined stiffness of the sample and gage. Second, the ISDG is noncontacting; the gage length is only 300 μm long, making it very difficult to physically attach a gage. Third, high precision is achieved; displacement must be measured to a resolution of 3 nm to measure 10 μstrain on a sample with a gage length of 300 μm. Strain is measured on two sides of the specimen to account for bending due to misalignment. Figure 5 shows stress-strain curves from a well-aligned sample (aligned within 5 μm) and a sample that shows significant bending effects (aligned within 32 μm). For both tests, the modulus calculated from the average strain on a steel sample was 190 GPa.

The motherboards that control the four arrays of photodiodes generate six output signals. Each array has a voltage output that corresponds to signal intensity. There is also a master clock and trigger signal shared by all the boards. The trigger gives a TTL output when the motherboard begins sampling the first pixel on the first array, and each pixel on successive diode arrays is sampled during one interval of

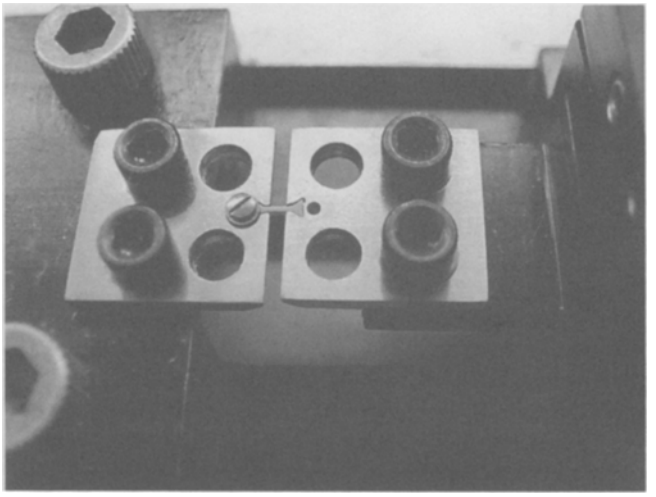
Fig. 3—A microsample in the grips. On the right-hand side, the air bearing is supporting the movable grip. One of the screws that trap the sample has been removed

the TTL clock. The clock typically is set to 5-10 kHz, but it could run much faster given a brighter laser source. The clock speed is adjusted before a test to maximize the fringe intensity without saturating the detector—the slower the scan rate, the greater the measured intensity. The input to the computer is then four arrays of integer values of the fringe intensity. Each array is 512 elements corresponding to the number of segments in the photodiode.

Data are acquired and processed in real time by a 12-bit computerized data acquisition system. The board is controlled by subroutines, supplied by the manufacturer, incorporated into MS-FORTRAN code. The computer is a 386-DX40 running MS-DOS.

The strain and load are recorded and processed in real time. The load is received as a voltage signal and converted using a linear calibration. Analyzing the strain is somewhat more complicated. For two-sided strain measurement, four sets of fringe patterns are monitored. An external clock signal provides the timing for the diode mother boards, which send a single start pulse followed by four arrays of data. Ten-point moving averages of each array are calculated to reduce noise and the effect of laser speckle. These cleaned arrays are sent to an algorithm that follows the central minimum and finds a best-fit parabola from the 15 points centered on the

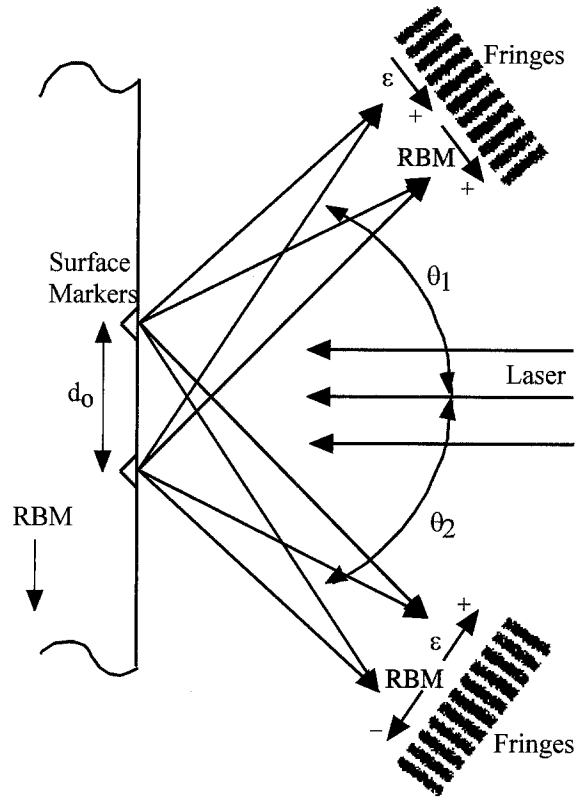

Fig. 4—Optical principle of the interferometric strain/displacement gage technique (RBM = rigid body motion)

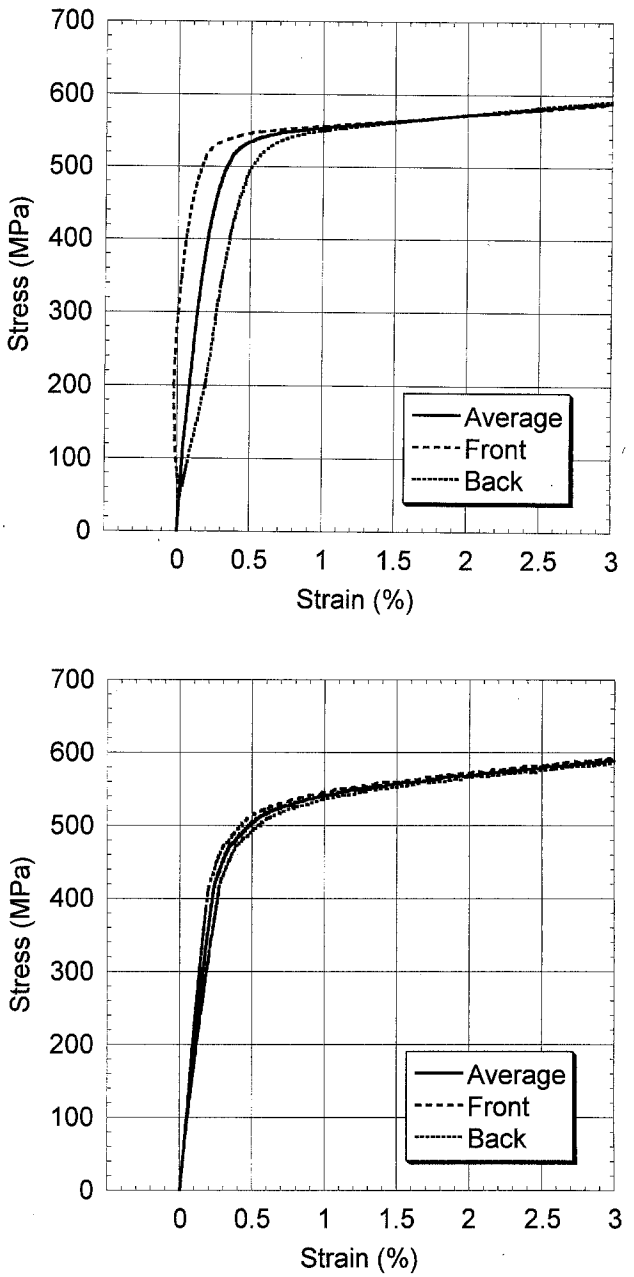

Fig. 5—Stress-strain curves showing front, back and average strain measurements for (a) a misaligned and (b) a well-aligned sample

pixel with lowest intensity. With this technique, the location of the minima is interpolated to a fraction of a pixel.[5] The phase shift is made dimensionless by dividing the shift in pixels from one cycle to the next by the spacing between two central, adjacent minimums. This dimensionless phase shift is independent of the distance between the sample and the detector, as well as the angle between the normal to the detector and the incoming fringe pattern. The phase shift is converted to strain; the readings from the two front and back diodes are averaged to remove rigid body motion, and the front and back measurements are averaged. Figure 6 shows the variation in strain and stress measurements; the data were subtracted from a linear fit to show the deviation. The standard deviation in the strain and stress measurements for a typical sample is 12 microstrain and 0.8 MPa.

Specimen Cutting and Preparation

Samples can be cut from large sections using several techniques. Thin slices are cut using a diamond saw or wire electric discharge machining. Samples were cut with a bench-top computerized numerical control (CNC) mill during the early stages of this project. This technique was used for the samples cut for the ASTM Cross-Comparison exercise discussed in the following section. Quantifying the amount of plastic deformation induced by machining is difficult. EDM cuts metal by applying a carefully controlled electric discharge to vaporize a small volume of metal in front of the electrode. The sample is not subjected to mechanical stress, but the outer surface is rapidly heated and cooled, and some molten metal redeposits on the cut surface. With a low energy and slow speed, this recast layer on steel can be reduced to just a few micrometers.[6] Tomlinson and Jupe,[7] Fu, Wu and Liu[8] and Nakamura *et al.*[9] have characterized the surface damage induced by EDM on brittle materials. The damage can be reduced to levels associated with grinding with 400-grit abrasive.

Sections of weldment 125 mm wide by 200 mm long by 51 mm thick fabricated at the Naval Surface Warfare Center–Carderock Division were delivered to Johns Hopkins University for testing. Slices were cut oversized to allow the recast layer and surface corrosion product to be ground away before further testing. Each of these sample coupons was ground with 320- through 1200-grit abrasive paper. The thickness

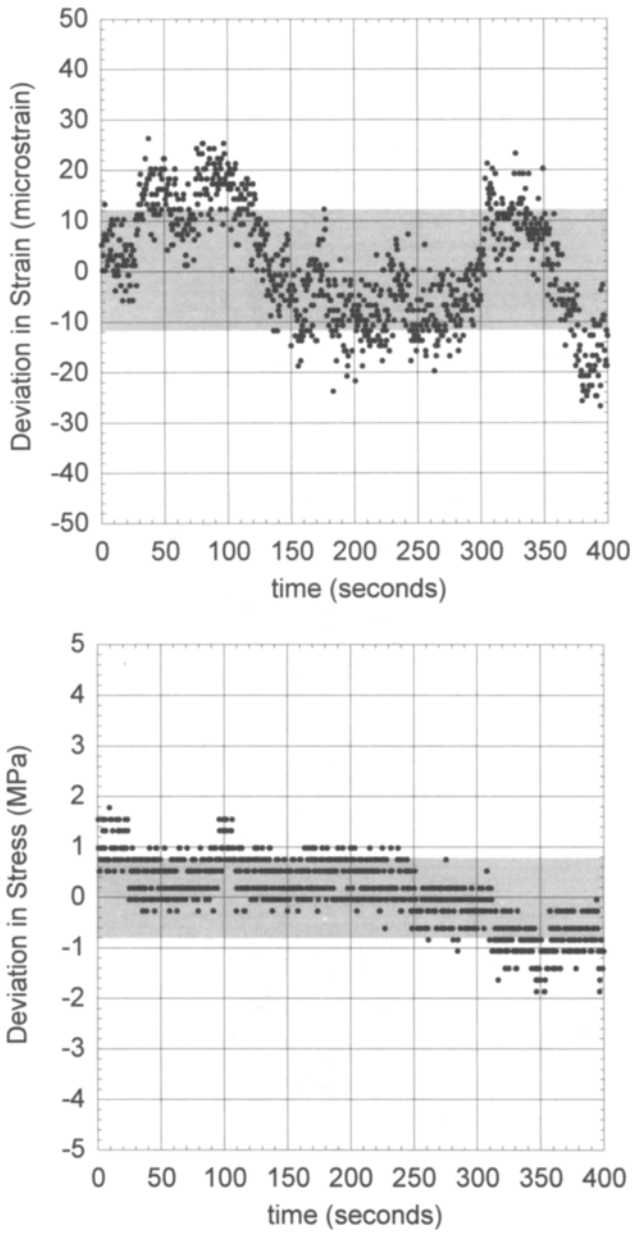

Fig. 6—Variation in measurements. (a) Interferometric strain/displacement gage: The highlighted region reflects plus and minus one standard deviation of 12 microstrain. (b) Stress for an average sample: One standard deviation is 0.8 MPa

after this stage was typically 200 to 250 μm. Hydrogen absorption was not monitored during this project, since typically it is not a concern for the ferritic weld metal, and since no brittle fracture was seen during testing. Next, microhardness scans were made on the sample coupons followed by macro etching with 3-percent NitAl to aid in finding the test locations.

The first group of samples was cut from the coupons using a sinking EDM with Microfinn surface finish enhancement. A "cookie-cutter" electrode was machined out of high-density, fine-grained graphite using a high-precision EDM with a 75 μm diameter wire. The electrode was designed so that the center section removed from the coupon during the cutting process was the sample. The sample coupons were glued to a steel block using a conductive variation of Crystal Bond™ adhesive developed for this project. After each sample was cut, the electrode was removed from the machine, refaced on 600-grit SiC paper to remove any rounding due to erosion on the end of the electrode and reinserted in the machine to cut another sample. Dielectric was flushed through the center of the electrode, which is a critical procedure to eliminate the contamination of the gap and the associated degradation in surface finish.

In later stages of the project, samples were cut in "six-packs" using an EDM with 250-μm hard-drawn brass wire. The dielectric fluid for this machine is chilled distilled water. The speed was typically 1000 μm/min, and the spark energy was reduced to 3. The CNC program was written to cut six samples at one time, ensuring that the centerline of all the samples coincided.

The samples were glued to small Pyrex disks with Crystal Bond™ adhesive, and small pieces of hard-drawn steel wire were mounted around the perimeter to help preserve the flatness of the specimen during polishing. The samples were ground very lightly with 400- through 1200-grit SiC paper. After each step, the samples were washed to remove any remaining abrasive and grinding debris; then, they were rotated 90 deg before proceeding to the next finer abrasive. Figure 7 shows a sample that was removed from the test machine after 5 percent of plastic deformation. The indents had no effect on the sample behavior; necking initiated at the center of the gage length. The roughness of the EDM surface also had no visible effect.

Development and Validation

The first-generation microsample test machine was constructed in 1992;[10] this machine supported the movable grip on soft springs and used a home-built load cell. The machine was modified to incorporate the linear air bearing and commercial load cell and was driven by a piezoelectric actuator for microsample fatigue studies.[11] A simpler

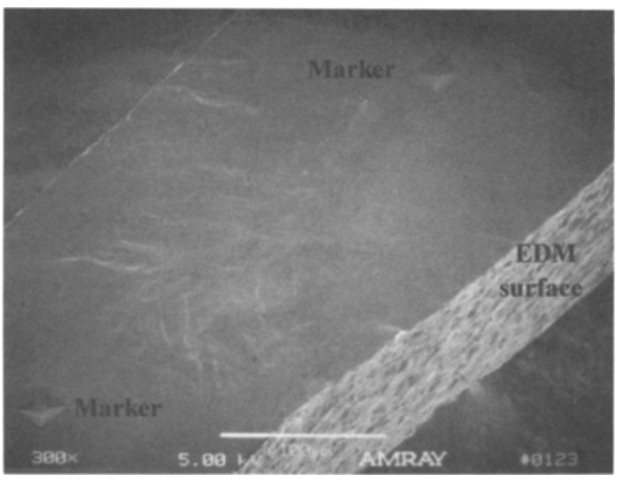

Fig. 7—Center section of a microsample that was removed after a few percent strain. Two microhardness markers, as well as slip lines, are evident on the polished top surface. The unpolished electric discharge machining (EDM) surface is visible in the foreground

version of this machine, with the piezoelectric actuator replaced by a screw drive, was used to test 47 steel samples as part of the ASTM Cross-Comparison in 1995, described in detail below.[12] The machine design was changed to incorporate two-sided strain measurement in 1996.[13] Since then, many samples of weld metal (this work), LIGA-nickel,[14,15] intermetallic single crystals,[16] nanomaterials[17] and silicates[18] have been tested.

Specimens of A533-B steel were tested as part of the ASTM Cross-Comparison Exercise on Determination of Material Properties Through the Use of Miniature Mechanical Testing Techniques. Each participant was supplied material from the same plate and asked to use his or her own techniques to measure the properties. Twenty-seven microspecimens oriented in the rolling direction were tested; the results are shown in Table 1. The average of the microsample results agrees to within a fraction of a percent with the macro results used as the baseline.[19] The force application and measurement system, as well as the strain measurement system, have been demonstrated to be valid when compared with traditional techniques.

Weld Description

Weld HBA was fabricated from MIL-70S filler metal on HY-100 plate with a gas metal arc weld (GMAW or MIG) process. The heat input was 65-70 kJ/in. The nominal strength of this filler metal is 483 MPa. Weld HBB was fabricated from MIL-100S filler metal on HY-100 plate; the heat input was 80 kJ/in., and the nominal yield is 690 MPa. Both welds are double-vee geometry with no root gap on 50.8-mm (2-in.) plate. Figure 8 shows the nominal design and a photo of the fabricated weld with test locations marked.

Weld Metal Results

Table 2 shows the tensile properties measured with full-sized specimens and the average results of the microspecimens tested at each site on the two welds. The full-sized, 12.5-mm diameter, all-weld-metal specimens report the average properties of several weld beads. The average of all the microsamples tested from the same region as the full-sized samples (the outer three sites) agree within 10 percent. The samples at the center of the weld showed considerably higher strength than those away from the center. Weld HBA showed a much larger variation from site to site, depending on whether the sample was in an as-deposited weld bead or weld metal heat-affected zone. The average strength at the center of the weld was 40 percent greater than nominal. Weld HBB showed only a small change from site to site; the strength at the center was 10 percent higher than nominal.

Several of the sites on weld HBA showed anisotropic behavior. The response, with respect to test orientation, for the location 23 mm from the center is listed in Table 3. Each of the three samples tested in the three orthogonal directions is listed, as well as the average for each direction. The yield strength in the longitudinal direction is close to the nominal value (483 MPa), but the yield in the transverse direction is 27 percent below that expected. The Vickers microhardness shows no significant variation.

TABLE 1—COMPARISON OF MICROTENSILE AND MACRO SAMPLES OF ASTM A533-B STEEL (DATA ARE REPORTED AS AVERAGE ± ONE STANDARD DEVIATION)

	0.2 Percent Yield (MPa)	Ultimate (MPa)
Microtensile	453 ± 24	609 ± 25
Macro	455	611

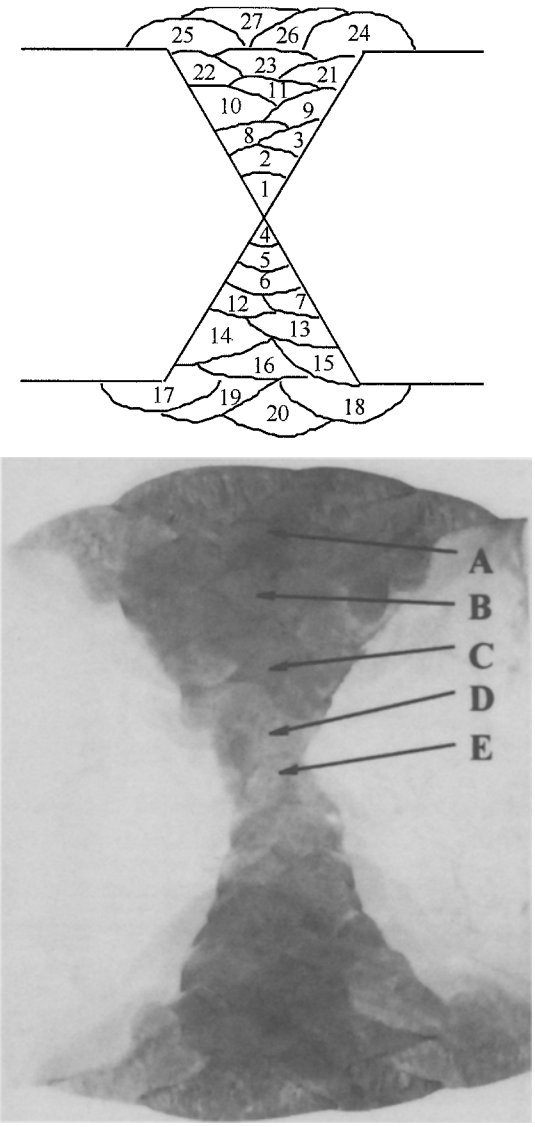

Fig. 8—Weld HBA: (a) nominal joint design and (b) a photo with test sites marked

Vickers microhardness measurements were made on all the samples. A linear correlation between microhardness and strength was established. This relationship did not account for directional variation because the microhardness measurements were not sensitive to the test orientation. Figures 9 and 10 are plots of the yield and ultimate as a function of Vickers microhardness. The graphs illustrate the broad scatter in this relationship; in general, the 95-percent confidence limits are ±100 MPa, and the distribution narrows at higher strengths and hardnesses. The results of microsamples from weld HBA, HBB and the HY-100 base plate all fall on the same line. The relationship for the yield strength agrees quite closely with the relationship of Pargeter[20] for matched weld metal on a steel similar to HY-80. The R^2 value for the

TABLE 2—UNDERMATCHED WELD METAL ON HY-100 PLATE (MACRO AND MICROTENSILE RESULTS, REPORTED AS AVERAGE ± ONE STANDARD DEVIATION)

Sample Description and Location		0.2 Percent Yield (MPa)	Ultimate (MPa)
Weld HBA	Macro	486 ± 12.4	607 ± 9.7
	23 mm from center	426 ± 59	569 ± 49
ESAB L-TEC 86	17 mm from center	443 ± 50	597 ± 40
MIL-70S-6	10 mm from center	466 ± 60	600 ± 30
	4 mm from center	550 ± 67	663 ± 36
	Center	675 ± 29	758 ± 28
Weld HBB	Macro	664 ± 38	751 ± 46
	22 mm from center	621 ± 41	775 ± 11
Lincolnweld LA-100	17 mm from center	621 ± 47	797 ± 14
MIL-100S-1	11 mm from center	607 ± 38	745 ± 12
	6 mm from center	690 ± 25	777 ± 12
	Center	756 ± 29	849 ± 21

TABLE 3—MICROSAMPLE TENSILE TEST RESULTS FOR THE OUTERMOST SITE ON WELD HBA

Sample	0.2 Percent Yield (MPa)	Average Yield	Ultimate (MPa)	Average Ultimate	Vickers Microhardness	Average Vickers
Longitudinal-1	508		651		187	
Longitudinal-2	483	481	593	605	179	185
Longitudinal-3	451		572		188	
Short Transv.-1	445		546		181	
Short Transv.-2	438	445	520	524	179	181
Short Transv.-3	451		507		182	
Transverse-1	343		539		187	
Transverse-2	343	353	635	578	191	187
Transverse-3	374		559		184	

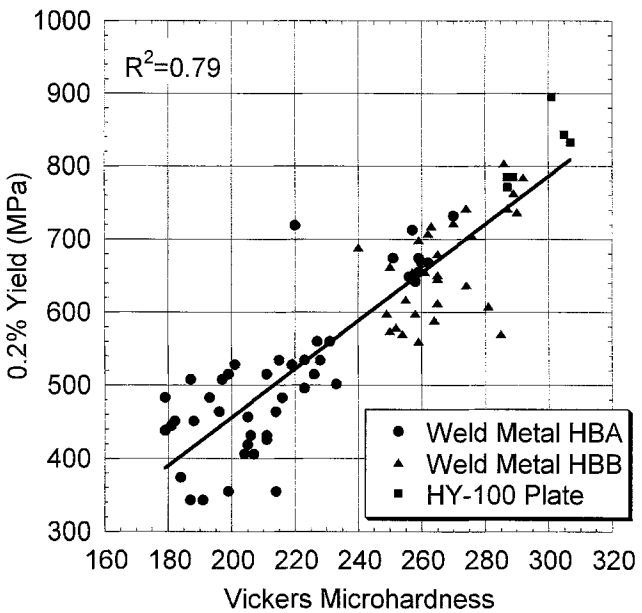

Fig. 9—0.2-percent yield versus Vickers microhardness

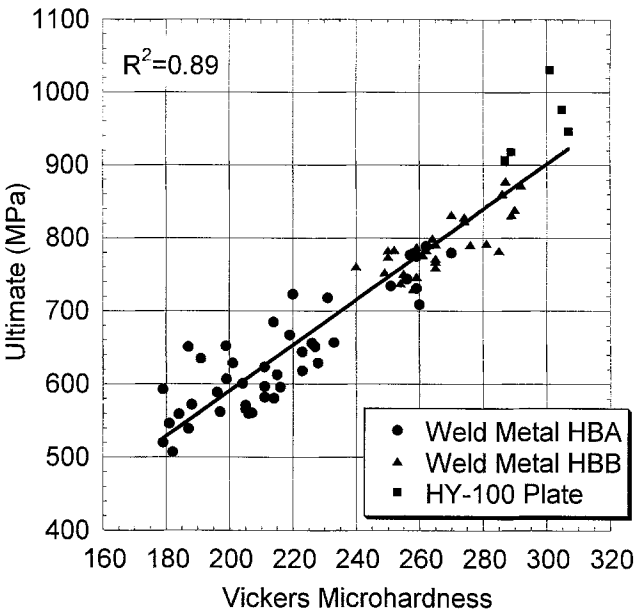

Fig. 10—Ultimate versus Vickers microhardness

correlation with ultimate strength is better than that for the correlation with yield strength. The relationships determined with microsamples are

$$\sigma_y(\text{MPa}) = 3.15H_v - 168(R^2 = 0.79)$$

$$\sigma_{uts}(\text{MPa}) = 2.84H_v + 28(R^2 = 0.89).$$

Conclusions

The microsample test technique accurately measures the modulus, yield strength and ultimate strength when compared to full-sized samples. It is capable of measuring variations in mechanical properties that depend on orientation of the loading direction while testing a very small region.

The results from the weld samples show that the properties vary considerably with location, with the samples from the

center of the weld being stronger than samples from the outer region. Some of the sites showed significant anisotropy as well.

Acknowledgments

The authors would like to acknowledge Bin Yuan for contributions to the development of this technique and George Coles and Greg Shoukas for performing the later series of tests. This work was supported by the Naval Surface Warfare Center–Carderock Division, with Robert Tregoning as project administrator.

References

1. Peterson, R.E., Stress Concentration Factors, Wiley-Interscience, New York (1974).

2. Sharpe, W.N., Jr., "The Interferometric Strain Gage," EXPERIMENTAL MECHANICS, **8** *(4), 164–170 (1968).*

3. Sharpe, W.N., Jr., "Applications of the Interferometric Strain/Displacement Gage," Opt. Eng., **21**, *483–488 (1982).*

4. Sharpe, W.N., Jr., "An Interferometric Strain/Displacement Measurement System," NASA Technical Memorandum 101638 (1989).

5. Sharpe, W.N., Jr., Zeng, H., Yuan, B., and Wallace, S., "A Technique for Microsample Testing of Weldments," Fracture '94, The Fourth National Conference on Fracture, Johannesburg (1994).

6. Lim, L.C., Lee, L.C., Wong, Y.S., and Lu, H.H., "Solidification Microstructure of Electrodischarge Machined Surfaces of Tool Steels," Mat. Sci. Tech., **7**, *239–248 (1991).*

7. Tomlinson, W.J. and Jupe, K.N., "Strength and Microstructure of Electrodischarge-machined Titanium Diboride," J. Mat. Sci. Lett., **12** *(6), 366–368 (1993).*

8. Fu, C.T., Wu, J.M., and Liu, D.M., "The Effect of Electrodischarge Machining on the Fracture Strength and Surface Microstructure of an AL2O3-Cr3C2 Composite," Mat. Sci. Eng. A, **A188**, *91–96 (1994).*

9. Nakamura, M., Shigematsu, I., Kanayama, K., and Hirai, Y., "Surface Damage in ZrB2-based Composite Ceramics Induced by Electro-discharge Machining," J. Mat. Sci., **1** *(26), 6078–6082 (1991).*

10. Sharpe, W.N., Jr. and Fowler, R.O., "A Novel Miniature Tension Test Machine," Small Specimen Test Techniques Applied to Nuclear Reactor Vessel Thermal Annealing and Plant Life Extension, ed. W. Corwin, F. Haggag and W. Server, ASTM STP 1204, Philadelphia, PA, 386–401 (1993).

11. Yuan, B. and Sharpe, W.N., Jr., "Fatigue Testing of Microspecimens," Fatigue '96, **III**, *Berlin, 1943–1948 (1996).*

12. Sharpe, W.N., Jr., Danley, D., and LaVan, D.A., "Microsample Tensile Tests of A533-B Steel," Small Specimen Test Techniques, ed. W.R. Corwin, S.T. Rosinski and E.V. Walle, ASTM STP 1397, West Conshocken, PA (1997).

13. LaVan, D.A. and Sharpe, W.N., Jr., "Strain Measurement on Miniature Tensile Samples," SEM Spring Conference on Experimental Mechanics, Bellevue, Washington (1997).

14. Sharpe, W.N., Jr., LaVan, D., and Edwards, R.L., "Mechanical Properties of LIGA-deposited Nickel for MEMS Transducers," IEEE 1997 International Conference on Solid-state Sensors and Actuators, Chicago, 607–610 (1997).

15. Sharpe, W.N., Jr., LaVan, D.A., and McAleavey, A., "Mechanical Testing of Thicker MEMS Materials," 1997 ASME Congress, Dallas (1997).

16. Zupan, M., LaVan, D., and Hemker, K.J., "Tensile and Compression Testing of Single-crystal Gamma-Ti-55.5 Al," 1996 MRS Fall Symposium: High Temperature Ordered Intermetallic Alloys VII, **460**, *Boston, 171–176 (1996).*

17. Legros, M., Hemker, K.J., LaVan, D.A., Sharpe, W.N., Jr., Rittner, M.N., and Weertman, J.R., "Micro-tensile Testing Nanocrystalline Al/Zr Alloys," 1996 MRS Fall Symposium: Nanophase and Nanocomposite Materials II, **457**, *Boston, 273–278 (1996).*

18. Noe, D., LaVan, D.A., and Veblen, D., "Lap-shear Testing of Biotite and Phlogopite Crystals and the Application of Interferometric Strain/Displacement Gages to Mineralogy," J. Geophys. Res.-Solid Earth (1999).

19. Rosinski, S.T. and Corwin, W.R., "ASTM Cross-comparison Exercise on Determination of Material Properties Through Miniature Sample Testing," Small Specimen Test Techniques, ASTM STP 1329, ed. W.R. Corwin, S.T. Rosinski and E. van Walle, American Society for Testing and Materials, Philadelphia, 3–14 (1998).

20. Pargeter, R.J., "Yield Strength from Hardness—A Reappraisal for Weld Metal," Welding Inst. Res. Bull. 325–326 (November 1978).